

Published in final edited form as:

Cancer Res. 2010 July 15; 70(14): 5860–5869. doi:10.1158/0008-5472.CAN-10-0726.

RUNX REGULATION OF SPHINGOLIPID METABOLISM AND SURVIVAL SIGNALLING

A. Kilbey^{1,*}, A. Terry¹, A. Jenkins¹, G. Borland¹, Q. Zhang², M.J.O. Wakelam², E.R. Cameron¹, and J.C. Neil^{1,*}

¹Molecular Oncology Laboratory, Institute of Comparative Medicine, Faculty of Veterinary Medicine, University of Glasgow, Glasgow, G61 1QH, United Kingdom

²The Babraham Institute, Babraham Research Campus, Cambridge, CB22 3AT, United Kingdom

Abstract

The *Runx* genes (*Runx1*, *2* and *3*) regulate cell fate in development and can operate as either oncogenes or tumour suppressors in cancer. The oncogenic potential of ectopic *Runx* expression has been demonstrated in transgenic mice that develop lymphoma in potent synergy with over-expressed *Myc*, and in established fibroblasts that display altered morphology and increased tumorigenicity. Candidate oncogenic functions of over-expressed *Runx* genes include resistance to apoptosis in response to intrinsic and extrinsic stresses. In a search for gene targets responsible for this aspect of *Runx* phenotype we have identified three key enzymes in sphingolipid metabolism (*Sgpp1*, *Ugcg* and *St3gal5/Siat9*) as direct targets for *Runx* transcriptional regulation, in a manner consistent with survival and apoptosis resistance. Consistent with these changes in gene expression, mass spectrometric analysis demonstrated that ectopic *Runx* reduces intracellular long chain ceramides in NIH3T3 fibroblasts and elevated extracellular sphingosine 1 phosphate (S1P). *Runx* expression also opposed activation of JNK and p38^{MAPK}, key mediators of ceramide-induced death, and suppressed the onset of apoptosis in response to exogenous TNF α . The survival advantage conferred by ectopic *Runx* could be partially recapitulated by exogenous S1P and was accompanied by reduced phosphorylation of p38^{MAPK}. These results reveal a novel link between transcription factor oncogenes and lipid signalling pathways involved in cancer cell survival and chemoresistance.

Keywords

RUNX; sphingolipid; ceramide; survival; apoptosis; TNF α

INTRODUCTION

The *Runx* genes comprise a three-membered family of mammalian transcription factors that regulate developmental cell fate decisions where cells are selected to proliferate, differentiate, survive or die. Unusually, these genes have been shown to act either as oncogenes or as tumor suppressors according to lineage and host cell genetic context (1). The transcriptional targets for *Runx* regulation are therefore of considerable interest and have already been shown to include factors involved in lineage-specific development as well as regulators of cell cycle checkpoints (2-4).

*Corresponding authors .

Notably, all three *Runx* genes have been implicated as oncogenes in lymphoid neoplasia in retroviral mutagenesis screens (5-8), while both Runx1 and Runx2 have been shown to be potently synergistic with Myc (9,10). The role of Runx in this context appears to be, at least in part, due to inhibition of Myc-induced apoptosis (11). Further evidence of an oncogenic role for Runx2 is provided by its ectopic expression in breast and prostate cancers where it is associated with metastasis and survival in the bone environment (12,13), while Runx1 promotes tumorigenicity in fibroblasts (14). Runx-mediated survival has also been reported *in vitro*. In lymphoid cells Runx1 confers resistance to apoptosis induced by CD3 ligation (15) or dexamethasone (4), while in fibroblasts all three *Runx* genes were shown to enhance survival under the stress of medium exhaustion (4,14).

Despite this evidence for potent pro-survival activity, the relevant pathways regulated by Runx are not well known. Our previous gene array analysis revealed a paucity of well-established regulators of apoptotic pathways among the significantly regulated targets. However, a set of 50 genes selected on the basis of significant regulation by all three Runx regulated genes included three genes encoding enzymes involved in sphingolipid metabolism (4). Each of these genes (*Sgpp1*, *Ugcg*, *St3gal5*(*Siat9*)) has been reported to play a role in regulating survival and apoptosis (16-18), suggesting that they may be important targets and determinants of Runx oncogenic potential. We now show that all three genes act as direct targets for Runx activation or repression. Moreover, biochemical analyses demonstrate that Runx expression causes significant changes in intracellular sphingolipids and resets the ceramide-sphingosine-1-phosphate “rheostat” (19) in favour of cell survival.

METHODS

Cell culture and transfections

NIH3T3 fibroblast-derived cells expressing *Runx1*, *Runx2* and *Runx3* genes from the pBabe retroviral vector system were maintained as previously described (4). Transfections were carried out using Superfect Transfection Reagent (Qiagen, Crawley, UK) according to the manufacturer’s instructions. Conditions for transfection have been previously described (4). Live/dead cell counts were carried out using a haemocytometer and Trypan blue as a vital indicator. Graphs were generated with Sigma-Plot and error bars relate to standard deviations. For TNF α experiments cells were treated with 10ng/ml TNF α (Peprotech Inc) in the presence of 10ug/ml cycloheximide (Sigma) for the indicated times.

Quantitative real-time PCR

Runx-expressing and control fibroblasts were grown to confluence in duplicate wells (7 days). Cells expressing the *RUNX1-ER* construct were treated for a further 1 – 24 hours with 4-OHT. cDNA preparation and the microarray assay were performed as described (4). For quantitative real-time PCR, aliquots (5ul) of cDNA were amplified in triplicate using primers for murine endogenous control *Hprt* or primers for murine *Sgpp1*, *St3gal5* (Qiagen QuantiTect Primer Assays) or *Ugcg* (779F 5’- tttgctcagtagctgctgaagatta 3’ and 861R 5’ acttgagtagacattgaaaacctccaa 3’) Relative quantification was carried out and calibrated to vector control samples (20).

Gel Retardation Analysis

DNA-binding reactions were performed as described previously (21) using 10ug of nuclear extracts and 4ng of ³²P-labelled double stranded oligonucleotide probe. Reactions were resolved by electrophoresis on 4% (w/v) 0.5x Tris-borate EDTA acrylamide gels at 4°C after which the gels were fixed and dried and complexes visualized by autoradiography. The following double stranded oligonucleotides were used as probes: *Sgpp1* site A -5’ ccttgagtagacattgaaaacctccaa 3’, *Sgpp1* Site Amut -5’ ccttgcatagcacagctgt 3’. Where indicated a

50x excess of cold competitor DNA or 2 μ l monoclonal Runx2 antiserum (MWG #D130-3) or Runx3 antiserum (a kind gift from Y. Ito) were added to the reaction 15min prior to the addition of the probe.

Luciferase Reporter Assays

Transcription assays were performed as described (22) using 2×10^5 cells per 60mm-diameter tissue culture dish. The assays shown are representative of at least 3 independent experiments carried out in duplicate. The luciferase activity was normalised to the protein concentration (Bio-Rad protein assay) present in each extract. pGL3Basic luciferase reporter (Promega) was used in all transcription assays. Expression of luciferase activity was driven by a 362bp fragment amplified from the murine *Sgpp1* promoter spanning two consensus Runx binding sites (-133 to -495). Site directed mutagenesis (QuikChange II Site-Directed Mutagenesis Kit – Stratagene) was used to generate base pair mutations in the distal site (gaccacag mutated to tagcacag) or in both sites (gaccacag mutated to tagcacag and caccgctg mutated to caccgctg) to determine efficacy of Runx mediated *Sgpp1* repression. pGL3control (Promega) which contains the SV40 promoter and enhancer driving the expression of the luciferase gene was included in all individual experiments to confirm similar levels of transfection efficiency between experiments.

Mass Spectrometry

Fibroblasts cell pellets ($\sim 2 \times 10^5$ cells) containing 15 ng C17-ceramide as an internal standard were extracted using a modified Folch method (extraction with 4ml Chloroform : 2ml methanol : 2ml 0.88% NaCl for each sample, followed by extraction of upper phase with 3ml of synthetic lower phase of chloroform/methanol/0.88% NaCl 2:1:1, the combined lower phases were dried under vacuum and redissolved in 50 μ l chloroform/methanol 1:1, 2 μ l was injected for LC-MS analysis). Cell culture media (4ml from $\sim 2 \times 10^5$ cells) containing 30 ng C17-sphingosine-1-phosphate as internal standard, concentrated to 1ml at room temperature under vacuum was extracted with 3×1 ml n-butanol, combined, concentrated and redissolved in 40 μ l methanol with 2 μ l injected for LC-MS analysis using a Shimadzu IT-TOF LC/MS/MS system. In detail, lipid classes of the Folch extract were separated on a normal phase silica gel column (100 \AA , 4 μ m, 150 \times 1mm, MicoSolv Technology) using a hexane/ dichloromethane/ chloroform/ methanol/ acetanitrile/ water/ ethylamine gradient based on the polarity of head group. Accurate mass (with mass accuracy ~ 5 ppm) and tandem MS were used for lipid molecular species identification and quantification. Lipid identity was further confirmed by reference to appropriate lipid standards. Mass spectrometer operation conditions: ESI interface voltage +4.0kv for positive ESI and -3.5kv for negative ESI, heat block temperature 210 $^{\circ}$ C, nebulising gas flow 1.0 L/min, CDL temperature 200C, with drying gas on. All the solvents used for lipid extraction and LC-MS analysis were LC-MS grade from FisherScientific.

Western blotting and antibodies

Preparation of whole cell protein extracts was performed as described previously (4). Samples equivalent to 50 μ g of protein (Bio-Rad protein assay) were resolved on 10% SDS-polyacrylamide gels and transferred to enhanced chemiluminescence (ECL; Amersham, Little Chalfont, UK) nitrocellulose membranes. The antibodies used were α Phospho-p38 MAPK 9211 (Cell Signaling Technologies) and α p38 MAPK (C20) sc535 (Santa Cruz Biotechnology).

In vitro JNK kinase Assay

Functional JNK activity was measured using a non radioactive SAPK/JNK Assay kit #9810 (Cell Signaling Technologies) according to the manufacturers instructions. Parallel lysates

all contained an equal concentration of protein (Bio-Rad protein assay). Immunoblotting was performed with an anti phospho-specific cJun (Ser63) antibody as supplied by the kit. The blot was re-probed against α GST(Z5) sc459 (Santa Cruz Biotechnology) to ensure equal loading of c-Jun (1-89) GST Fusion protein beads.

Caspase 3 detection of Apoptosis

Activated caspase 3 was detected using an activated caspase 3 assay kit (#550914, BD Biosciences) according to the manufacturer's instructions; 10,000 events per sample were analysed on an Epics XL flow cytometer (Beckman Coulter) using Expo32 software.

RESULTS

Key enzymes in sphingolipid metabolism are direct targets for Runx regulation

In a previous study we compared the global transcriptional changes in immortalised fibroblasts expressing ectopic Runx1, 2 or 3. In contrast to primary fibroblasts, which enter a state of senescence-like growth arrest in response to Runx (14,20,23,24), these cells undergo a characteristic phenotypic change resembling mesenchymal to epithelial transition and display greatly enhanced survival in response to stresses including medium exhaustion (4). Gene expression microarray analysis revealed a largely overlapping set of target genes with no evidence of genes that were oppositely regulated by each of the three family members. In a common Runx signature set defined by the 50 most significantly regulated genes, we found a preponderance of genes encoding cell surface molecules or secreted factors, but few candidates with an annotated role in control of apoptosis. However, gene ontology analysis indicated a bias towards a small set of genes encoding enzymes involved in sphingolipid metabolism that were of potential significance in this regard (4).

In this study we have examined Runx regulation of the three sphingolipid enzymes and assessed its potential significance for Runx-mediated survival and oncogenesis. Figure 1A shows the biochemical steps catalysed by the respective enzymes. The right-hand side of the figure shows the fold-change in mRNA levels induced by constitutive expression of Runx1, Runx2 or Runx3 in 3T3 fibroblasts as measured by Affymetrix gene expression microarray (<http://www.ncbi.nlm.nih.gov/geo/query/acc.cgi?acc=GSE11732>) and validated by quantitative real-time PCR. UDP-glucose ceramide glycosyltransferase (*Ugcg*) and ST3 beta-galactoside alpha-2,3-sialyltransferase 5 (*St3gal5/Stat9/GM3* synthase) are both markedly up-regulated by Runx gene expression, while sphingosine-1-phosphate phosphatase 1 (*Sgpp1*) is down-regulated. The lower panel (Figure 1B) shows a kinetic analysis of the mRNA levels after activation of an inducible RUNX1-ER construct. The fact that the observed regulation happens rapidly supports the hypothesis that all three genes act as direct transcriptional targets for the *Runx* genes, with *Ugcg* and *St3gal5* as targets for activation, while *Sgpp1* is repressed. As a further test for direct regulation we examined the requirement for protein synthesis by inducing RUNX1-ER in the presence of cycloheximide. Although interpretation of these experiments was complicated by the non-specific effects of cycloheximide on the stability of some transcripts it was clear that *Ugcg* induction and *Sgpp1* repression were insensitive to cycloheximide inhibition. *St3gal5* induction was preserved at very early time points but lost after 6 hours due to the non-specific stabilisation of transcripts by cycloheximide (Supplementary Figure 1).

Screening of the promoter regions of the three genes revealed consensus Runx binding sites close to the transcriptional start site in each case. *St3gal5* has three discrete sites (-602, -1151, -1834), while *Ugcg* has one site (-345) and *Sgpp1* has two closely linked sites (-416, -348). The *Sgpp1* promoter region is the most highly conserved sequence across mammalian species and also contains conserved E box motifs next to the proximal site (B).

As shown in Figure 2A, chromatin immunoprecipitation confirmed Runx binding at each of these sites. Runx2 expressing cells were employed in this instance to take advantage of antibodies suitable for use under ChIP conditions.

In view of the evidence that Sgpp1 plays a central role in regulation of the ceramide-S1P rheostat and cell survival we focused further efforts on validating the regulatory consequences of Runx binding. We confirmed that Runx proteins from nuclear extracts bound specifically to both site A and site B in EMSA (Figure 2B and data not shown). A luciferase expression construct with a basal promoter under control of the *Sgpp1* regulatory element (-133 to -495) showed negative regulation in the presence of ectopic Runx, that was reduced by mutation of site A and abolished in the double mutant (Figure 2C). Basal levels of the double mutant were similar to those of the wild-type promoter in the absence of ectopic Runx expression, suggesting that steady state levels of Runx in fibroblasts are too low to cause significant repression.

Ceramide and S1P levels are modulated by Runx

To explore the biochemical consequences of altered transcription of genes encoding sphingolipid enzymes, we examined the ceramide/S1P profiles by mass spectrometry in the presence and absence of ectopic Runx. Levels of extracellular S1P were found to be essentially undetectable in serum-free cultures of control cells. However, whilst the data were somewhat variable, we were able to detect S1P in the culture medium of cells expressing Runx with values ranging from 0 to 0.88 ng S1P/ 5ml culture medium of 2×10^5 cells cultured serum free. In contrast, we consistently observed a marked reduction in the level of several long chain ceramides in the presence of ectopic Runx (Figure 3A). Ceramides 16:0, 24:1 and 24:0 are typical of the salvage pathway of ceramide synthesis, suggesting that Runx expression opposes sphingosine recycling via this route (17). The most dramatic effect observed was on the levels of 16.0 ceramide (Figure 3A) which has previously been reported to respond to Sgpp1 expression and is implicated as a critical component of ceramide-induced apoptosis (17,25,26).

Runx expression reduces stress-associated kinase signalling

To investigate the consequences of long chain ceramide depletion for Runx-dependent cell survival, we examined the functional activity of p38^{MAPK} and JNK which play central roles in stress-induced cell death and apoptotic signalling by ceramide (27-29). For this purpose, NIH3T3 fibroblasts expressing ectopic Runx1 or control vector were grown under conditions of medium exhaustion and adherent cells harvested every 1-3 days for analysis of phospho-p38^{MAPK} expression and JNK activity. Consistent with our previous data (4), expression of ectopic Runx conferred protection against stress-induced cell death under these growth conditions (Figure 3B). Furthermore, Runx-dependent cell survival correlated with reduced activation of the p38^{MAPK} and JNK signalling pathways as measured by accumulation of phosphorylated p38^{MAPK} and c-Jun respectively (Figures 3C & 3D).

Runx delays TNF α -induced cell death

TNF α has been reported to induce cell death through an accumulation of intracellular ceramide and downstream activation of the JNK signalling pathway (28). To determine whether this response is modified by ectopic Runx1, we examined the effects of TNF α on the survival of vector control and Runx1-expressing NIH3T3 fibroblasts. Cycloheximide (CHX) was included in short term assays to suppress the synthesis of short lived anti-apoptotic proteins that can reduce the effects of TNF α (30). As shown in Figure 4A morphological differences were observed as early as 2- 4 hours after TNF α and CHX treatment, with vector control cells rounding up and detaching from the substratum far more readily than their Runx1 expressing counterparts. Quantitation of adherent and non-adherent

cells by trypan blue exclusion confirmed greater survival in the presence of ectopic Runx1 (Figure 4B). The effect was exaggerated after 5 hours exposure to TNF α and CHX (Figure 4B) but lost by 24 hours when widespread cell death was observed throughout (data not shown). To determine whether Runx1 was protecting against apoptosis, FACS analysis was performed on caspase 3 labelled cells grown in the presence and absence of TNF α for longer time periods. A highly significant difference between Runx and control cultures was observed from the earliest time point out to 48 hours (Figure 4C), with Runx expressing cells showing a marked resistance to induction of caspase 3 over the time course.

These data suggest that modulation of sphingolipid enzymes by ectopic Runx resets the sphingolipid rheostat against intracellular ceramide-induced apoptosis and in favour of cell survival.

Runx survival is partially reproduced by exogenous S1P

The reduction of intracellular ceramide in Runx expressing cells may be due to the cumulative action of the three target enzymes leading to synthesis of glycosylated forms or gangliosides (Ugcg, St3gal5) or to accumulation of S1P (Figure 5). S1P functions as a lipid signal that can promote proliferation and suppress ceramide-mediated apoptosis. S1P is actively transported outside the cell where it signals through a family of G-protein coupled receptors. In addition, S1P appears to be able to act via as yet uncharacterised intracellular receptors (31). Although the detection of extracellular S1P was variable in Runx expressing fibroblasts it is probable that this pathway is constitutively activated since other pathways of S1P removal are found in cells and S1P was essentially undetectable in control cultures. To explore this hypothesis we tested whether Runx-expressing cells retained sensitivity to growth regulation by exogenous S1P. NIH3T3 fibroblasts expressing ectopic Runx1 or control vector were grown to confluence and cultured under conditions of medium exhaustion for 8 days in the presence or absence of increasing concentrations of S1P. Viability counts were then performed on detached cells in the supernatant and the adherent cultures harvested to determine the phosphorylation status of p38^{MAPK}.

As shown in Figure 6A, exogenous S1P reduced cell death in a dose dependent manner in both cell backgrounds but the effect was more pronounced in the absence of ectopic Runx1, supporting the proposal that S1P signalling was already activated by elevated S1P generation in the Runx expressing fibroblasts. Cell viability counts confirmed this trend, with the difference between Runx expressing and control cultures reduced to only 3% in the presence of 10⁻⁶ M S1P (Figure 6B). These data support previous studies in NIH3T3 fibroblasts showing a reduction in stress-induced apoptosis in the presence of exogenous S1P (32). Furthermore, the improved survival of control cultures correlated with reduced expression levels of phosphorylated p38^{MAPK} (Figure 6C). At higher doses of S1P, expression levels of phospho p38^{MAPK} were comparable to those in the Runx expressing cultures which were relatively refractory to S1P (Figure 6C). These data suggest that while p38^{MAPK} inhibition correlates with improved cell survival of control cultures, ectopic expression of Runx has already saturated the relevant survival pathway.

DISCUSSION

Over-expression of *Runx* genes has context-specific effects, inducing growth arrest or senescence in most primary cell types, but promoting proliferation and/or survival in cells expressing collaborating oncogenes or mutated tumor suppressor pathways (1,14,24,24,33). In NIH3T3 fibroblasts, which lack Cdkn2a (Ink4a/Arf) function, over-expression of Runx potently induces survival under stress conditions. Our previous exploration of the likely effector genes in this phenotype revealed a paucity of candidates with established roles in apoptosis or survival, with the notable exception of a small set of genes involved in

sphingolipid metabolism that were over-represented as a gene ontology subset (4). In this study we have demonstrated that the *Runx* genes can directly regulate three genes encoding enzymes with central roles in sphingolipid pathways (Figure 5). Of particular note is the ability of all three *Runx* genes to repress expression of *Sgpp1*, a key player in the sphingosine rheostat that governs the interchange between pro-apoptotic ceramides (34) and S1P, a well-established ligand in survival signalling (19). Moreover, ectopic Runx expression was shown to drive a major reduction in the level of specific intracellular ceramide species, a finding that was associated with reduced induction of stress-associated p38^{MAPK} and JNK activity. The selective reduction in a subset of ceramide species points to these lipids as being specific substrates for Ugcg and also suggests that these particular ceramides signal through specific target proteins to mediate pro-apoptotic effects. The selective action of particular species within a lipid class has been previously recognised for diacylglycerol and phosphatidic acid (35). Resistance to death induced by TNF α , which operates via ceramide, was also confirmed in Runx expressing cells, while the Runx associated survival phenotype could be at least partially recapitulated by addition of exogenous S1P. These results suggest that modulation of sphingolipid metabolism underlies the oncogenic and pro-survival effects of ectopic Runx expression in multiple contexts (4,11,15) and indicates the possibility of a wider role for Runx in cancer chemoresistance.

Published studies provide strong support for the hypothesis that the three novel Runx target genes we have described play a significant role in the observed survival phenotype. For example, RNAi knockdown of *Sgpp1* expression was shown to promote cell survival with concomitant accumulation of intracellular and extracellular S1P, while ectopic expression of *Sgpp1* was reported to drive the conversion of S1P to long chain ceramides and a subsequent apoptotic response (32). Ectopic expression of Ugcg has been reported to rescue cells from ceramide-induced apoptosis (16). Furthermore, multidrug resistance of breast cancer cell lines has been associated with the shunting of ceramide into a glucosyl ceramide sink and can be reversed by siRNA or oligonucleotide blockade of Ugcg (36). The effects of up-regulation of *St3gal5* are less readily predicted, as high levels of GM3 are associated with the induction of apoptosis in some cancer cells (18), whereas re-introduction of *St3gal5* into lines that fail to synthesize GM3 was shown to enhance their ability to form colonies in soft agar and increase their resistance to stress induced apoptosis (37). We suggest that the outcome may reflect the steady state levels of GM3 in different cellular backgrounds. In this regard it is notable that upregulation of *Ugcg* by Runx is much more marked than *St3gal5* and that glycosylation of ceramide is also a key step in the synthesis of cerebrosides and gangliosides other than GM3.

Improved survival of Runx expressing fibroblasts also correlated with reduced levels of intracellular long-chain ceramides. The induction of apoptosis through ceramide production is complex, involving both direct and indirect modes of action and multiple signalling pathways. Mitochondrial damage and caspase release is driven by the formation of ceramide channels in the mitochondrial membrane (38) but also through the activation of stress activated kinases such as p38^{MAPK}, which further activate pro-apoptotic Bax and Bak, and inhibit anti-apoptotic Bcl2 and Bcl-XL (39). It has been suggested that the solubility of these target molecules enables ceramide at non-mitochondrial locations such as the ER membranes to participate in the apoptotic process (40). Notably, we observed reduced steady-state p38^{MAPK} phosphorylation and JNK activity in stressed cells expressing ectopic Runx and both of these kinase pathways have been reported to be induced by intracellular ceramide (29,39). Further evidence of a role for sphingolipid-mediated changes in the Runx survival phenotype was provided by the greater resistance of Runx-expressing cells to TNF α -induced apoptosis, that has also been reported to operate via ceramide and JNK signalling pathways (29).

It is notable that we were able to partially recapitulate the survival phenotype of Runx expressing cells via exogenous administration of S1P to control cells. S1P can mediate survival by binding to a series of cell surface receptors (reviewed in (41)) but can also act by a less well characterised intracellular route (17). The variable detection of free S1P in the medium of Runx expressing cells could suggest that the latter route is operative here. Nevertheless, it appears that S1P pathways are fully engaged in these Runx-expressing cells, as exogenous S1P caused no additional survival benefit in this context. Sgpp1 is not the only plasma membrane-located enzyme able to degrade S1P, there being a family of lipid phosphate phosphatases (LPPs) able to hydrolyse a range of signalling lipids including S1P and LPA (42). The LPPs appear to be regulated by substrate availability, thus whilst a reduction in Sgpp1 could reduce the degradation of S1P in the proximity of the S1P receptor following its release from the cell, it will not necessarily induce sustained elevation of medium S1P concentration. In support of this it was reported that reduced expression levels of LPP1 in ovarian cancer cells was not accompanied by a corresponding increase in extracellular LPA (43).

The involvement of sphingolipid enzymes in cancer and chemo-resistance (27,44) suggest a wider role for Runx in these phenomena, and our results establish a link between previous reports of the *Runx* genes as targets for retroviral activation in an *in vivo* model of acquired imatinib resistance in CML (45) and studies showing that imatinib resistance can be conferred through changes in the ceramide-S1P rheostat (46). Moreover, the ability of Runx to confer metastatic potential may be mediated by the ability to promote close adhesion (4,14) and sphingolipid-mediated cell survival under adverse conditions *in vivo*. Finally, the *Runx* genes have been widely studied as essential players in lineage-specific differentiation in which they can act as both positive and negative regulators of proliferation according to context (47-49). The possibility that these regulatory steps are mediated through sphingolipid metabolism merits further investigation.

Supplementary Material

Refer to Web version on PubMed Central for supplementary material.

Acknowledgments

We thank Dr S. Wotton for helpful comments and discussions. This work was supported with a joint programme grant from Cancer Research UK and Leukaemia and Lymphoma Research to the Molecular Oncology Laboratory. Lipidomic analyses were performed at the Babraham Institute and supported by grants from Cancer Research UK and the BBSRC (MJOW).

References

1. Blyth K, Cameron ER, Neil JC. The Runx gene family : gain or loss of function in cancer. *Nat Rev Cancer*. 2005; 5:376–87. [PubMed: 15864279]
2. Lutterbach B, Hiebert SW. Role of the transcription factor AML-1 in acute leukemia and hematopoietic differentiation. *Gene*. 2000; 245:223–35. [PubMed: 10717473]
3. Otto F, Lubbert M, Stock M. Upstream and downstream targets of RUNX proteins. *J Cell Biochem*. 2003; 89:9–18. [PubMed: 12682904]
4. Wotton S, Terry A, Kilbey A, et al. Gene array analysis reveals a common Runx transcriptional programme controlling cell adhesion and survival. *Oncogene*. 2008; 27:5856–66. [PubMed: 18560354]
5. Stewart M, Terry A, Hu M, et al. Proviral insertions induce the expression of bone-specific isoforms of PEBP2alphaA (CBFA1): evidence for a new myc collaborating oncogene. *Proc Natl Acad Sci USA*. 1997; 94:8646–51. [PubMed: 9238031]

6. Wotton S, Stewart M, Blyth K, et al. Proviral insertion indicates a dominant oncogenic role for Runx1/AML1 in T-cell lymphoma. *Cancer Res.* 2002; 62:7181–5. [PubMed: 12499254]
7. Stewart M, Mackay N, Cameron ER, Neil JC. The common retroviral insertion locus Dsi1 maps 30kb upstream of the P1 promoter of the murine Runx3/Cbfa3/Aml2 gene. *J Virol.* 2002; 76:4364–9. [PubMed: 11932403]
8. Lund AH, van Lohuizen M. RUNX: A trilogy of cancer genes. *Cancer Cell.* 2002; 1:213–5. [PubMed: 12086855]
9. Vaillant F, Blyth K, Terry A, et al. A full length Cbfa1 gene product perturbs T-cell development and promotes lymphomagenesis in synergy with MYC. *Oncogene.* 1999; 18:7124–34. [PubMed: 10597314]
10. Blyth K, Terry A, Mackay N, et al. Runx2: a novel oncogenic effector revealed by in vivo complementation and retroviral tagging. *Oncogene.* 2001; 20:295–302. [PubMed: 11313958]
11. Blyth K, Vaillant F, Mackay N, et al. *Runx2* and *MYC* collaborate in lymphoma development by suppressing apoptotic and growth arrest pathways *in vivo*. *Cancer Res.* 2006; 66:2195–201. [PubMed: 16489021]
12. Pratap J, Javed A, Barnes GL, et al. Runx2 regulates tumor cell invasive properties and contributes to the osteolytic bone disease associated with metastatic cancer cells. *Journal of Bone and Mineral Research.* 2005; 20:16.
13. Barnes GL, Javed A, Waller SM, et al. Osteoblast-related transcription factors Runx2 (Cbfa1/AML3) and MSX2 mediate the expression of bone sialoprotein in human metastatic breast cancer cells. *Cancer Res.* 2003; 63:2631–7. [PubMed: 12750290]
14. Wotton S, Blyth K, Kilbey A, et al. RUNX1 transformation of primary embryonic fibroblasts is revealed in the absence of p53. *Oncogene.* 2004; 23:5476–86. [PubMed: 15133495]
15. Fujii M, Hayashi K, Niki M, et al. Overexpression of AML1 renders a T hybridoma resistant to T cell receptor-mediated apoptosis. *Oncogene.* 1998; 17:1813–20. [PubMed: 9778047]
16. Bleicher RJ, Cabot MC. Glucosylceramide synthase and apoptosis. *Biochimica et Biophysica Acta-Molecular and Cell Biology of Lipids.* 2002; 1585:172–8.
17. Le Stunff H, Galve-Roperh I, Peterson C, Milstien S, Spiegel S. Sphingosine-1-phosphate phosphohydrolase in regulation of sphingolipid metabolism and apoptosis. *J Cell Biol.* 2002; 158:1039–49. [PubMed: 12235122]
18. Watanabe R, Ohyama C, Aoki H, et al. Ganglioside G(M3) overexpression induces apoptosis and reduces malignant potential in murine bladder cancer. *Cancer Res.* 2002; 62:3850–4. [PubMed: 12097299]
19. Maceyka M, Payne SG, Milstien S, Spiegel S. Sphingosine kinase, sphingosine-1-phosphate, and apoptosis. *Biochimica et Biophysica Acta-Molecular and Cell Biology of Lipids.* 2002; 1585:193–201.
20. Kilbey A, Blyth K, Wotton S, et al. *Runx2* disruption promotes immortalization and confers resistance to oncogene-induced senescence in primary murine fibroblasts. *Cancer Res.* 2007; 67:11263–71. [PubMed: 18056452]
21. Kilbey A, Black EJ, Unlu M, Gillespie DAF. The v-Jun oncoprotein replaces p39 c-Jun as the predominant AP-1 constituent in ASV17-transformed fibroblasts: Implications for SAPK/JNK-mediated signal transduction. *Oncogene.* 1996; 12:2409–18. [PubMed: 8649782]
22. Taylor ER, Boner W, Dornan ES, Corr EM, Morgan IM. UVB irradiation reduces the half-life and transactivation potential of the human papillomavirus 16 E2 protein. *Oncogene.* 2003; 22:4469–77. [PubMed: 12881703]
23. Kilbey A, Terry A, Cameron ER, Neil JC. Oncogene induced senescence: an essential role for Runx. *Cell Cycle.* 2008; 7:2333–40. [PubMed: 18677118]
24. Wolyniec K, Wotton S, Kilbey A, et al. RUNX1 and its fusion oncoprotein derivative RUNX1-ETO induce senescence-like growth arrest independently of replicative stress. *Oncogene.* 2009; 28:2502–12. [PubMed: 19448675]
25. Kolesnick R, Hannun YA. Ceramide and apoptosis. *Trends in Biochemical Sciences.* 1999; 24:224–5. [PubMed: 10366847]

26. Le Stunff H, Giussani P, Maceyka M, Lepine S, Milstien S, Spiegel S. Recycling of sphingosine is regulated by the concerted actions of sphingosine-1-phosphate phosphohydrolase 1 and sphingosine kinase 2. *J Biol Chem.* 2007; 282:34372–80. [PubMed: 17895250]
27. Oskoui B, Sooriyakumaran P, Borowsky AD, et al. Sphingosine-1-phosphate lyase potentiates apoptosis via p53- and p38-dependent pathways and is down-regulated in colon cancer. *Proc Natl Acad Sci USA.* 2006; 103:17384–9. [PubMed: 17090686]
28. Cuvillier O. Sphingosine in apoptosis signaling. *Biochimica et Biophysica Acta-Molecular and Cell Biology of Lipids.* 2002; 1585:153–62.
29. Verheij M, Bose R, Lin XH, et al. Requirement for ceramide-initiated SAPK/JNK signalling in stress-induced apoptosis. *Nature.* 1996; 380:75–9. [PubMed: 8598911]
30. Jin S, Ray RM, Johnson LR. TNF- α /cycloheximide-induced apoptosis in intestinal epithelial cells requires Rac1-regulated reactive oxygen species. *American Journal of Physiology-Gastrointestinal and Liver Physiology.* 2008; 294:G928–G937. [PubMed: 18218673]
31. Spiegel S, Milstien S. Sphingosine-1-phosphate: An enigmatic signalling lipid. *Nature Reviews Molecular Cell Biology.* 2003; 4:397–407.
32. Mandala SM, Thornton R, Galve-Roperh I, et al. Molecular cloning and characterization of a lipid phosphohydrolase that degrades sphingosine-1-phosphate and induces cell death. *Proc Natl Acad Sci USA.* 2000; 97:7859–64. [PubMed: 10859351]
33. Linggi B, Muller-Tidow C, van de LL, et al. The t(8;21) fusion protein, AML1 ETO, specifically represses the transcription of the p14(ARF) tumor suppressor in acute myeloid leukemia. *Nat Med.* 2002; 8:743–50. [PubMed: 12091906]
34. Obeid LM, Linardic CM, Karolak LA, Hannun YA. Programmed Cell-Death Induced by Ceramide. *Science.* 1993; 259:1769–71. [PubMed: 8456305]
35. Hodgkin MN, Pettitt TR, Martin A, Michell RH, Pemberton AJ, Wakelam MJO. Diacylglycerols and phosphatidates: which molecular species are intracellular messengers? *Trends in Biochemical Sciences.* 1998; 23:200–4. [PubMed: 9644971]
36. Zhang XF, Li J, Qiu ZG, Gao P, Wu XJ, Zhou GY. Co-suppression of MDR1 (multidrug resistance 1) and GCS (glucosylceramide synthase) restores sensitivity to multidrug resistance breast cancer cells by RNA interference (RNAi). *Cancer Biology & Therapy.* 2009; 8:1117–21. [PubMed: 19502811]
37. Uemura S, Kabayama K, Noguchi M, Igarashi Y, Inokuchi J. Sialylation and sulfation of lactosylceramide distinctly regulate anchorage-independent growth, apoptosis, and gene expression in 3LL Lewis lung carcinoma cells. *Glycobiology.* 2003; 13:207–16. [PubMed: 12626418]
38. Siskind LJ. Mitochondrial ceramide and the induction of apoptosis. *Journal of Bioenergetics and Biomembranes.* 2005; 37:143–53. [PubMed: 16167171]
39. Chen CL, Lin CF, Chang WT, Huang WC, Teng CF, Lin YS. Ceramide induces p38 MAPK and JNK activation through a mechanism involving a thioredoxin-interacting protein-mediated pathway. *Blood.* 2008; 111:4365–74. [PubMed: 18270325]
40. Simon CG, Holloway PW, Gear ARL. Exchange of C-16-ceramide between phospholipid vesicles. *Biochemistry.* 1999; 38:14676–82. [PubMed: 10545193]
41. Pyne S, Pyne N. Sphingosine 1-phosphate signalling via the endothelial differentiation gene family of G-protein-coupled receptors. *Pharmacology & Therapeutics.* 2000; 88:115–31. [PubMed: 11150592]
42. Brindley DN, Pilquil C. Lipid phosphate phosphatases and signaling. *Journal of Lipid Research.* 2009; 50:S225–S230. [PubMed: 19066402]
43. Tanyi JL, Hasegawa Y, Lapushin R, et al. Role of decreased levels of lipid phosphate phosphatase-1 in accumulation of lysophosphatidic acid in ovarian cancer. *Clin Cancer Res.* 2003; 9:3534–45. [PubMed: 14506139]
44. Liu YY, Yu JY, Yin DM, et al. A role for ceramide in driving cancer cell resistance to doxorubicin. *Faseb Journal.* 2008; 22:2541–51. [PubMed: 18245173]
45. Miething C, Grundler R, Mugler C, et al. Retroviral insertional mutagenesis identifies RUNX genes involved in chronic myeloid leukemia disease persistence under imatinib treatment. *Proc Natl Acad Sci USA.* 2007; 104:4594–9. [PubMed: 17360569]

46. Baran Y, Salas A, Senkal CE, et al. Alterations of ceramide/sphingosine 1-phosphate rheostat involved in the regulation of resistance to imatinib-induced apoptosis in K562 human chronic myeloid leukemia cells. *J Biol Chem.* 2007; 282:10922–34. [PubMed: 17303574]
47. Theriault FM, Nuthall HN, Dong ZF, et al. Role for Runx1 in the proliferation and neuronal differentiation of selected progenitor cells in the mammalian nervous system. *Journal of Neuroscience.* 2005; 25:2050–61. [PubMed: 15728845]
48. Pratap J, Galindo M, Zaidi SK, et al. Cell growth regulatory role of Runx2 during proliferative expansion of preosteoblasts. *Cancer Res.* 2003; 63:5357–62. [PubMed: 14500368]
49. Levanon D, Bettoun D, Harris-Cerruti C, et al. The Runx3 transcription factor regulates development and survival of TrkC dorsal root ganglia neurons. *EMBO Journal.* 2002; 21:3454–63. [PubMed: 12093746]

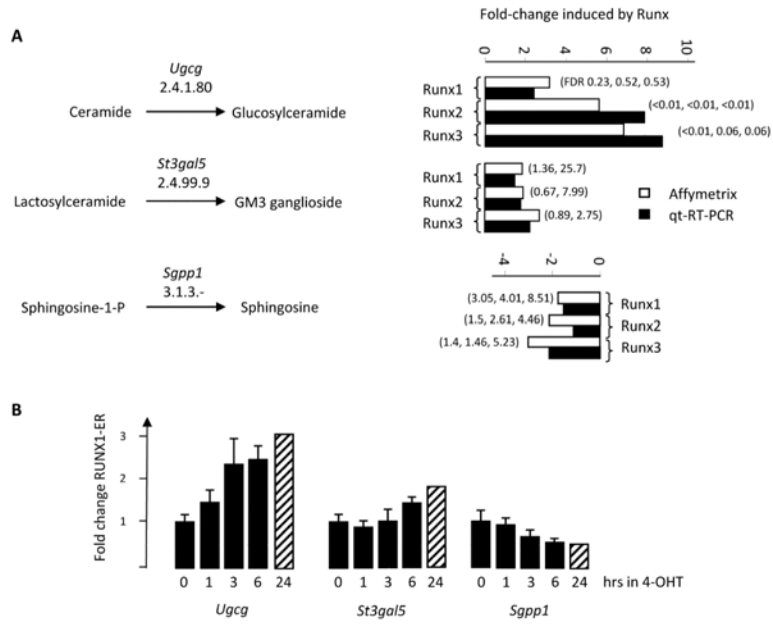


Figure 1. Functions of Runx regulated genes in lipid metabolism and validation of microarray data analysis. **(A)** Biochemical steps catalysed by Runx gene targets involved in sphingolipid metabolism and their respective Enzyme Commission numbers. Validation of array data for selected target genes by quantitative real-time PCR (qt-RT-PCR; SYBR green). Adjacent bars show fold regulation as measured by Affymetrix array and qt-RT-PCR. False discovery rate estimates for the individual gene probe sets on the Affymetrix chips are indicated. **(B)** Kinetic analysis of mRNA levels of each enzyme after activation of an inducible RUNX1-ER construct.

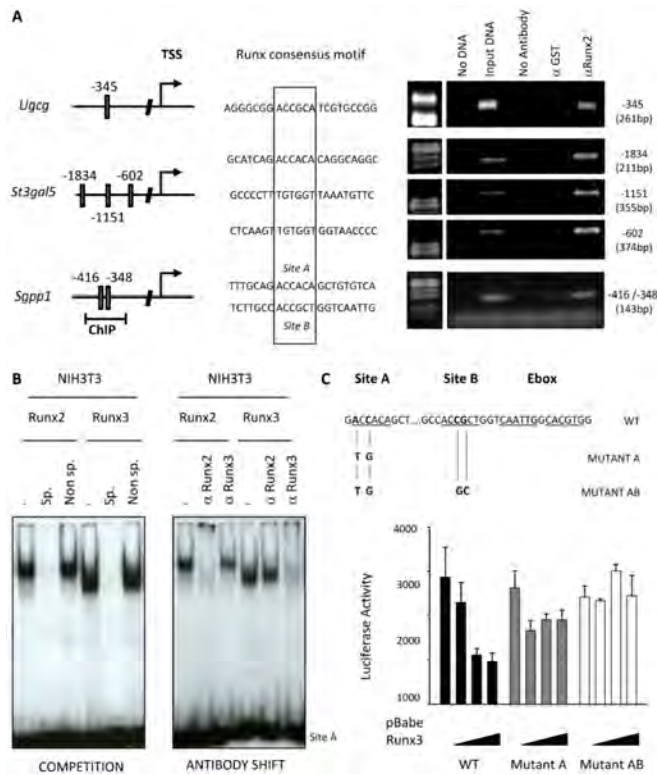
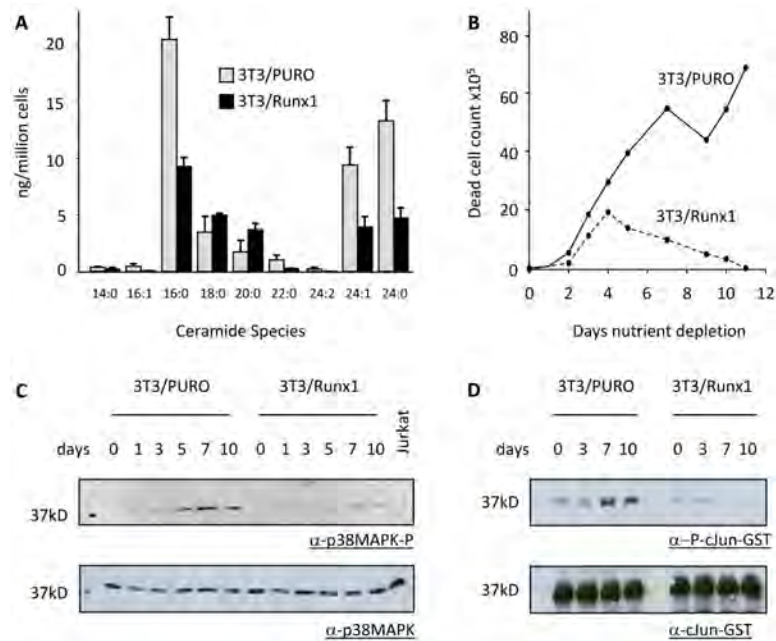


Figure 2. (A) Runx2 occupancy of promoter regions of *Ugcg*, *St3gal5* and *Sgpp1* *in vivo* as assessed by ChIP analysis. Specificity was demonstrated by lack of site recognition by a negative control polyclonal antiserum, α GST or when primary antibody was not included in the immunoprecipitation reaction. (B) DNA mobility shift assay using Runx consensus *Sgpp1* oligonucleotide A from the *Sgpp1* promoter and nuclear lysates prepared from Runx2 or Runx3 expressing NIH3T3 fibroblasts. Specificity of binding was indicated using excess cold competitor oligonucleotides and monoclonal antibodies specific for Runx2 or Runx3. (C) The ability of Runx to trans-repress the *Sgpp1* regulatory element is dependent on two Runx consensus motifs in the *Sgpp1* promoter. The data is representative of three independent transient transfections into HEK-293T cells and is normalised to the protein concentration present in the extract.

**Figure 3.**

(A) The ceramides in cultures of Puro vector control and Runx1 expressing NIH3T3 fibroblasts were extracted, separated, identified and semi-quantitated by HPLC_{mass} spectrometry. The data are means \pm SD where n=3 from one experiment typical of three. (B) Puro vector control and Runx1 expressing NIH3T3 fibroblasts were grown under conditions of medium exhaustion for 10 days. Dead cell counts were determined each day by trypan blue exclusion. (C). On the indicated days adherent cells from the same cultures were lysed and probed against antibodies to phospho-p38^{MAPK} or p38^{MAPK} as a loading control. (D) Parallel cell pellets were lysed for immunoprecipitation and incubated with c-Jun (1-89) GST fusion protein beads. Functional JNK activity was quantified in the presence of ATP by immunoblotting with a phospho specific antibody to c-Jun (Ser 63).

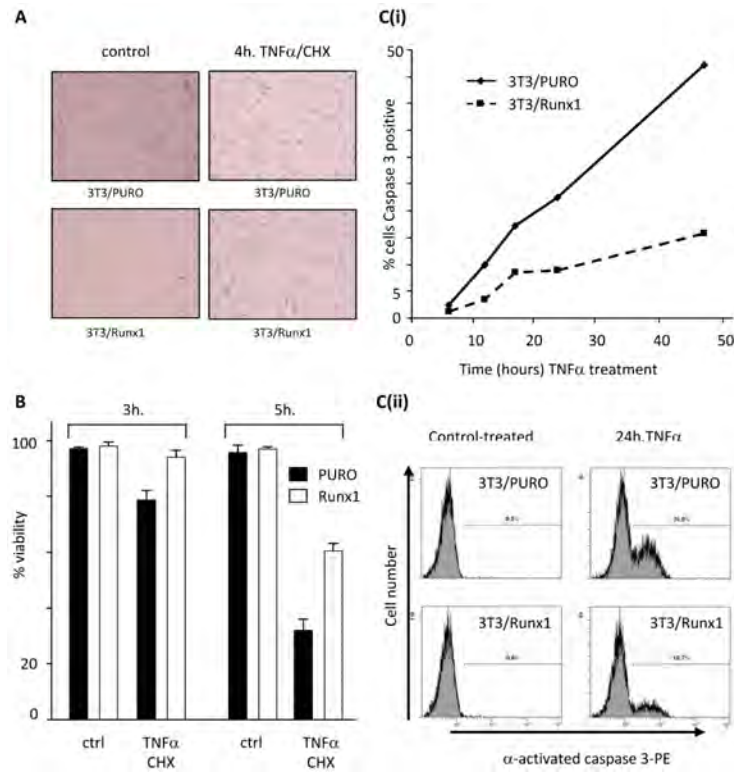


Figure 4.

(A) Puro vector control and Runx1 expressing fibroblasts were grown in the presence and absence of 10ng/ml TNF α and 10ug/ml CHX for up to 4 hours. Cultures were photographed every 2 hours. (B) Adherent and non adherent cells from parallel cultures were harvested after 3 and 5 hours TNF α /CHX treatment and viability counts performed by Trypan blue exclusion. (Ci) Cells treated with 10ng/ml TNF α alone for up to 48 hours were stained for intracellular activated caspase 3 and analysed by FACS at 6, 12, 17, 24 and 48 hours; (Cii) representative histogram plots showing caspase 3 activation in control and TNF α -treated cells at 24h.

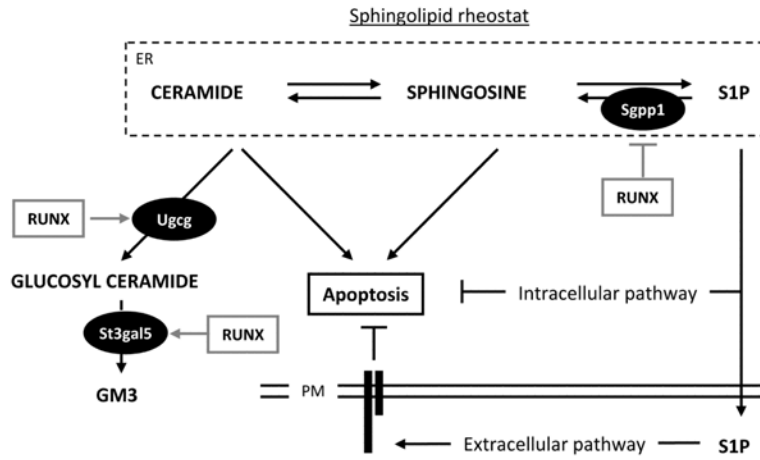


Figure 5. A model depicting the sphingolipid rheostat and the enzyme activities of three Runx gene targets relative to the central exchange of intracellular ceramide and S1P. The dynamic balance is normally tightly regulated and has direct consequences for cell survival and apoptosis.

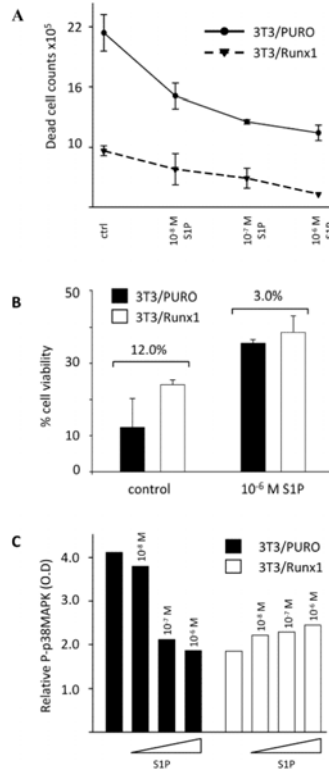


Figure 6. S1P signalling enhances cell survival and p38^{MAPK} dephosphorylation in control fibroblasts but is effectively silenced in the presence of ectopic Runx1. Confluent cultures were grown under conditions of nutrient starvation for 8 days in the presence of increasing concentrations of S1P. The data are representative of two independent experiments. **(A)** Day 8 dead cell suspension counts quantified by Trypan blue exclusion. **(B)** Corresponding viability counts showing the reduced survival advantage of Runx expressing fibroblasts compared to control cultures in the presence of extracellular S1P. **(C)** Adherent cells from the same cell cultures were harvested and analysed for phosphorylated p38^{MAPK} expression by western blotting using a phosphospecific p38^{MAPK} antibody. Levels are expressed relative to the total p38^{MAPK} loading control.